Available online at www.sciencedirect.com
ScienceDirect
Journal of Sound and Vibration 311 (2008) 597–607
JOURNAL OF SOUND AND VIBRATION
www.elsevier.com/locate/jsvi

On the growth and decay of transverse acceleration waves on a nonlinear, externally damped string

P.M. Jordan

Code 7181, Naval Research Laboratory, Stennis Space Ctr., MS 39529–5004, USA

Received 8 December 2006; received in revised form 31 August 2007; accepted 20 September 2007
Available online 5 November 2007

Abstract

We examine the growth and decay of transverse acceleration waves on a nonlinear string whose motion takes place in a resisting medium. It is shown that one effect of external damping is to increase, with respect to the undamped case, the rate at which growth/decay of the wave's amplitude takes place. In addition, the effects of the string's initial velocity are examined, a stability analysis is carried out, and a series of numerical simulations of acceleration waves on a finite string are presented.
Published by Elsevier Ltd.

1. Introduction

The study of what is referred to today as singular surfaces [1,2], i.e., wavefronts, across which some physical quantity of interest suffers a jump discontinuity, can be traced back to the 1848 paper by Stokes entitled "On a difficulty in the theory of sound" (see, e.g., the book by Johnson and Cheret [3]). What is most interesting about such waves, in particular the subclass known as *acceleration waves* [4], is the fact that under certain conditions, the jump amplitude can exhibit *finite-time blow-up*, also known as gradient catastrophe" [5] in the mathematical literature, even when the initial data are smooth. It is now generally thought that the blow-up of a transverse acceleration wave's amplitude implies the formation of a *vortex sheet*,[1] i.e., a propagating jump in the velocity component *parallel* to the wavefront [1,2,6]. However, as Coleman and Gurtin [7] have pointed out, there is no general mathematical proof of this conjecture; see, however, Fu and Scott [8], as well as the references therein.

The study of acceleration waves has been, and remains, a topic of great interest in many areas of the physical sciences. This is especially true in the field of continuum mechanics, where numerous works detailing cases of finite-time blow-up appear in the literature (see, e.g., Refs. [2,4,6–16] and those therein).

In the present paper, we examine the evolution of acceleration waves that can arise on a one-dimensional (1D) string that is executing finite-amplitude, transverse vibrations in a resisting medium. This study, which generalizes that of Jordan and Puri [13] to include the effects of external damping, employs both analytical and

E-mail address: pjordan@nrlssc.navy.mil

[1]The blow-up of a longitudinal acceleration wave's amplitude is thought to imply the formation of a *shock wave*, i.e. a propagating jump in the velocity component perpendicular to the wavefront [4].

0022-460X/$ - see front matter Published by Elsevier Ltd.
doi:10.1016/j.jsv.2007.09.024

numerical methods and shows that the primary effect of external damping is, in addition to causing attenuation of the solution profile, to increase the rate at which growth/decay of the acceleration wave's amplitude takes place. Additionally, the important role played by the string's initial velocity in determining if finite-time blow-up will occur is investigated.

To this end, the present article is arranged as follows. In Section 2, the equation of motion is derived. In Section 3, expressions for the acceleration wave's speed and amplitude are analytically determined using singular surface theory. Then, in Section 4, numerical simulations are presented to illustrate the analytical findings. Lastly, in Section 5, results are summarized, followed by the Appendix, wherein (jump) amplitude stability is discussed.

2. Equation of motion

Consider a homogeneous, elastic string of constant cross-sectional area A_0, which is the cross-sectional area in the undeformed configuration, that is executing transverse vibrations in a resisting medium, wherein the drag force is proportional to the string's velocity. Taking the x-coordinate of a (Cartesian) coordinate system along the length of the string and denoting the z-component of the displacement vector by u, let us assume that the motion of the string is confined to the xz-plane; i.e., the displacement vector of the string depends only on x and (time) t and its y-component is identically zero. If we also assume, as is typical in such problems, that $\tau \ll EA_0$, where τ denotes the tension and the positive constant E is Young's modulus, then longitudinal inertial effects are, in general, negligibly small; see [17, Section 3]. Consequently, the tension can be expressed in terms of u_x via Hooke's law [18,19]

$$\tau = \tau_0 - EA_0[1 - \sqrt{1 + (u_x)^2}], \tag{1}$$

where the positive constant τ_0 is the tension in the undisturbed string and x and/or t subscripts denote partial differentiation.

Applying Newton's second law to any element of string yields

$$\rho_0 u_{tt} = (\tau \sin\theta)_x - \varkappa u_t, \tag{2}$$

where the product $\tau \sin\theta$ gives the vertical component of the tension, the positive constants ρ_0 and $\varkappa$ denote the mass per unit length of the string in the undeformed configuration and the damping coefficient, respectively, and θ denotes the inclination of the tangent at any point on the string.

If we further assume that $|u_x| \ll 1$, then Eq. (1) and $\sin\theta$ can be approximated by $\tau \approx \tau_0 + \frac{1}{2}EA_0(u_x)^2$ and $\sin\theta \approx u_x[1 - \frac{1}{2}(u_x)^2]$. Consequently,

$$\tau \sin\theta = \frac{\tau u_x}{\sqrt{1 + (u_x)^2}} \approx \tau_0 u_x[1 + \beta(u_x)^2]. \tag{3}$$

Here, we have replaced $\frac{1}{2}(\tau_0^{-1}EA_0 - 1)$ with β, where $\beta = \frac{1}{2}\tau_0^{-1}EA_0$, since $EA_0 \gg \tau$ implies $EA_0 \gg \tau_0$ [17]. Substituting Eq. (3) into Eq. (2) yields, after simplifying, the equation of motion

$$u_{tt} + (\varkappa/\rho_0)u_t - c_0^2 u_{xx} = c_0^2\beta[(u_x)^3]_x, \tag{4}$$

where $c_0 = \sqrt{\tau_0/\rho_0}$ is the speed of shear waves according to the linear theory.

Since we are mainly interested in the behavior of the string at, and in the immediate vicinity of, an acceleration wave, let us now recast the equation of motion in terms of v, the z-component of $\mathbf{v}$, where $\mathbf{v} = (0, 0, v(x, t))$ denotes the velocity vector. To this end, we first apply $\partial/\partial t$ to Eq. (4) and then make use of the fact that $v = u_t$ to obtain

$$v_{tt} + (\varkappa/\rho_0)v_t - c_0^2 v_{xx} = 3c_0^2\beta[(u_x)^2 v_x]_x. \tag{5}$$

Employing next the wavefront approximation $u_x \approx -c_0^{-1}v$, which is also known as the "linear-impedance assumption" in the context of acoustics (see, e.g., Ref. [14] and those therein), to eliminate u_x, we find that in terms of v, the equation of motion becomes

$$v_{tt} + (\varkappa/\rho_0)v_t - c_0^2 v_{xx} = 3\beta(v^2 v_x)_x. \tag{6}$$

Introducing the following nondimensional variables: $v' = v/v_0$, $x' = x/\ell$, and $t' = t(c_0/\ell)$, where the positive constants v_0 and ℓ, respectively, denote a characteristic speed and length, Eq. (6) is reduced to

$$v_{tt} + \sigma v_t - v_{xx} = 3\varepsilon^2\beta(v^2 v_x)_x, \tag{7}$$

where $\varepsilon = v_0/c_0$ plays the role of the Mach number, the positive constant $\sigma = \varkappa\ell(\rho_0\tau_0)^{-1/2}$ is the (dimensionless) damping coefficient, and all primes have been omitted but are understood.

Before leaving this section the following remarks are in order. Firstly, we observe that with the damping term omitted, Eq. (4) is equivalent to Ref. [20, Eq. (2)]. Secondly, it should be noted that in finite-amplitude problems involving a finite-length string with fixed ends, some authors have replaced the quantity inside the [ ] in Eq. (1) with $-\mathscr{E} = (L - S)/L$, where $\mathscr{E}$ is the average Lagrangian strain [21], S is the length of the string in general, and L is the length of the string in its undisturbed state [i.e., $L = \min(S)$]; see Refs. [17,21] and those therein. And lastly, while the present study focuses on an externally damped string, it is appropriate to mention that other authors have considered internally damped (i.e., viscoelastic) strings, for which the tension is often described by the Kelvin–Voigt model (see, e.g., Refs. [22–24]).

3. Growth/decay of transverse acceleration waves

In carrying out the analytical part of our study, it is convenient to treat the acceleration waves as being kinematic [25], rather than dynamic, wave phenomena. Mathematically, this means recasting Eq. (7) as a system consisting of a "conservation/balance law" and a "flux" relation. That this is possible can be seen by setting $v = \Phi_x$ and $q = -\Phi_t$, where $\mathbf{P} = (0, \Phi(x,t), 0)$ is the vector velocity potential (i.e., $\mathbf{v} = \nabla \times \mathbf{P}$). Omitting the details, it is not difficult to establish that Eq. (7) is equivalent to the quasilinear system

$$\begin{pmatrix} v \\ q \end{pmatrix}_t + \mathbf{B}\begin{pmatrix} v \\ q \end{pmatrix}_x = -\sigma\begin{pmatrix} 0 \\ q \end{pmatrix}, \quad \text{where } \mathbf{B} = \begin{pmatrix} 0 & 1 \\ 1 + 3\beta\varepsilon^2 v^2 & 0 \end{pmatrix}. \tag{8}$$

Clearly, the eigenvalues of the coefficient matrix $\mathbf{B}$ are $\lambda_{1,2} = \pm\mathscr{C}(v)$, where $\lambda_{1,2}$ are the roots of the quadratic equation $\det(\mathbf{B} - \lambda\mathbf{I}_2) = 0$, $\mathbf{I}_2$ denotes the 2×2 identity matrix, and $\mathscr{C}(v) = \sqrt{1 + 3\beta\varepsilon^2 v^2}$. Since $\lambda_{1,2} \in \mathbb{R}$ and $\lambda_1 \neq \lambda_2$, it follows that this system is also *strictly hyperbolic* [5], with characteristics defined by $\mathrm{d}x/\mathrm{d}t = \pm\mathscr{C}(v)$.

Let us now assume that v and q are both continuous jointly in x and t, but that v_t suffers a jump (discontinuity) across the plane $t = 0$, i.e., at start-up. Due to the hyperbolic nature of system (8), planar wavefronts, across which v_t is discontinuous, begin propagating to the left and right along the x-axis at time $t = 0+$, the speed of each with respect to an observe at rest denoted here by $|U|(\neq 0)$. With no loss in generality, let us limit our attention to the right-traveling front, which we denote by $x = \Sigma(t)$, and for simplicity let us also take $\Sigma(0) = 0$. Mathematically, our assumptions can be restated as $[\![v]\!] = [\![q]\!] = 0$, but $[\![v_t]\!] \neq 0$. Here, the amplitude of the jump in a function $F = F(x,t)$ across Σ is defined as

$$[\![F]\!] \equiv F^- - F^+, \tag{9}$$

where $F^{\mp} \equiv \lim_{x \to \Sigma(t)^{\mp}} F(x,t)$ are assumed to exist and a " +" superscript corresponds to the region into which Σ is advancing while a "−" superscript corresponds to the region behind Σ. Such a wavefront, which is singular with respect to v_t *and* propagating along the string, is termed a (transverse) acceleration wave [4].

Hence, observing that $[\![v_t]\!]$ is, at most, a function of only t, and assuming that the value of $[\![v_t]\!]$ is known at time $t = 0$, we now seek to analytically determine the value(s) of U and the behavior of $[\![v_t]\!]$ for all $t > 0$.

The first step in the process is employing Hadamard's lemma [4,26]

$$\frac{\delta[\![F]\!]}{\delta t} = [\![F_t]\!] + U[\![F_x]\!], \tag{10}$$

where the 1D displacement derivative $\delta/\delta t$ gives the time-rate-of-change measured by an observer traveling with Σ, along with the assumptions $[\![v]\!] = [\![q]\!] = 0$, to obtain the jump relations

$$[\![v_t]\!] + U[\![v_x]\!] = 0, \quad [\![q_t]\!] + U[\![q_x]\!] = 0. \tag{11}$$

Next, we take the jumps of the two equations in system (8), which is permissible since the two equations are assumed to hold on both sides of Σ. This yields, after using the formula for the jump of a

product $[\![FG]\!] = F^+[\![G]\!] + G^+[\![F]\!] + [\![F]\!][\![G]\!]$ and simplifying, the two additional jumps equations

$$[\![v_t]\!] + [\![q_x]\!] = 0, \quad [\![q_t]\!] + \{1 + 3\beta\varepsilon^2(v^+)^2\}[\![v_x]\!] = 0, \tag{12}$$

where we have again used the assumption $[\![v]\!] = 0$. Our third step is to determine U. This is accomplished by setting the determinant of the coefficient matrix of this system of (four) jumps equations to zero. As a result, we obtain the propagation condition $U^2 - \mathscr{C}^2(v^+) = 0$, and thus it follows that $U = \pm\mathscr{C}(v^+)$. Taking the positive solution for obvious reasons, it is clear that Σ corresponds to the right-traveling wavefront $x = \mathscr{C}(v^+)t$.

Using Hadamard's lemma, system (8), and the jump relations given above, it is a straightforward process to show that the acceleration jump amplitude satisfies the Bernoulli equation

$$\frac{\delta a}{\delta t} + \left(\frac{\sigma}{2}\right)a - \left[\frac{3\beta\varepsilon^2 v^+}{1 + 3\beta\varepsilon^2(v^+)^2}\right]a^2 = 0, \tag{13}$$

where $a(t) \equiv [\![v_t]\!]$. Solving using standard methods, the exact solution is readily found to be

$$a(t) = \begin{cases} a(0)\exp\left(-\dfrac{1}{2}\sigma t\right), & v^+ = 0, \\ \dfrac{\alpha^*}{1 - [1 - \alpha^*/a(0)]\exp\left(\dfrac{1}{2}\sigma t\right)}, & v^+ \neq 0, \end{cases} \tag{14}$$

where

$$\alpha^* = \frac{\sigma[1 + 3\beta\varepsilon^2(v^+)^2]}{6\beta\varepsilon^2 v^+}. \tag{15}$$

From Eq. (14), we see that, from a purely mathematical standpoint, the temporal evolution of $a(t)$ can occur in any one of the following five possible ways:

(I) If $v^+ = 0$, then $a(t) \to 0$ from above (resp. below) for $a(0) > 0$ (resp. $a(0) < 0$) as $t \to \infty$.
(II) If $v^+ \neq 0$ and $a(0) = \alpha^*$, then $a(t) = \alpha^*$ for all $t \geqslant 0$.
(III) If $v^+ \neq 0$ and $\alpha^*/a(0) > 1$, then $a(t) \to 0$ from above (resp. below) for $\mathrm{sgn}(\alpha^*) = 1$ (resp. $\mathrm{sgn}(\alpha^*) = -1$) as $t \to \infty$.
(IV) If $v^+ \neq 0$ and $a(0)\alpha^* < 0$, then $a(t) \to 0$ from above (resp. below) for $\mathrm{sgn}(\alpha^*) = -1$ (resp. $\mathrm{sgn}(\alpha^*) = 1$) as $t \to \infty$.
(V) If $v^+ \neq 0$ and $\alpha^*/a(0) \in (0, 1)$, then $\lim_{t \to t_\infty} |a(t)| = \infty$, where the *breakdown* time $t_\infty (> 0)$ is given by

$$t_\infty \equiv \frac{2}{\sigma}\ln\left[\frac{a(0)}{a(0) - \alpha^*}\right]. \tag{16}$$

Here, we observe that the constant α^*, which is known as the *critical amplitude* [4] of the acceleration wave, is such that $\mathrm{sgn}(\alpha^*) = \mathrm{sgn}(v^+)$, where $v^+ \neq 0$ is naturally assumed. Also, some authors (see, e.g., Ref. [27]) refer to Σ as weak if $|a(0)| < |\alpha^*|$ and strong if $|a(0)| > |\alpha^*|$. Note too that when v^+ is zero, $a(t)$ reduces to the jump amplitude expression predicted by the linear theory [26]. More importantly, however, is the fact that Case (II) describes an *unstable* solution of Eq. (13) since any discrepancy, however small, in the value of $a(0)$ yields either Case (III) or (V); see the Appendix.

4. Analytical and numerical results for a model system

4.1. Problem formulation and analytical results

To illustrate the most important analytical findings of Section 3, we now present a series of numerical simulations based on the following simple (dimensionless) initial–boundary value problem (IBVP)

involving Eq. (7):

$$v_{tt}+\sigma v_t-v_{xx}=3\varepsilon^2\beta(v^2v_x)_x,\quad (x,t)\in(0,1)\times(-\infty,t_{\mathrm{r}});$$

$$v(0,t)=v^+-(-1)^pH(t)\sin(\Omega t),\quad v(1,t)=v^+,\quad t<t_{\mathrm{r}};\tag{17}$$

$$v(x,0)=v^+,\quad v_t(x,0)=0,\quad x\in(0,1);$$

where $H(\cdot)$ is the Heaviside unit step function; the positive constant t_{r} denotes the time of first reflection off the boundary $x=1$, i.e., t_{r} is the time required for Σ to complete its initial transit of the interval $(0,1)$; the constants $\Omega(>0)$ and v^+ denote the frequency of the sinusoidal excitation and the z-component of the string's initial velocity, respectively; and $p\in\{0,1\}$. Also, it should be noted when IBVP (17) is expressed in terms of dimensional quantities, v_0 and ℓ, our characteristic speed and length from Section 1, represent the magnitude of the sinusoidal excitation and the length of the string in the undeformed configuration, respectively.

Using the fact that $[\![v_x]\!]=-\mathscr{C}^{-1}(v^+)a(t)$, which follows from Eq. $(11)_1$, we can easily establish that an initial jump in v_t gives rise to a jump in v_x of amplitude

$$[\![v_x]\!]=\begin{cases}\Omega(-1)^p\exp\left(-\dfrac{1}{2}\sigma t\right), & v^+=0,\\[2ex] \dfrac{-\alpha^*[1+3\beta\varepsilon^2(v^+)^2]^{-1/2}}{1-[1+\alpha^*/\Omega(-1)^p]\exp\left(\dfrac{1}{2}\sigma t\right)}, & v^+\neq 0,\end{cases}\tag{18}$$

where the initial jump amplitude is given by $a(0)=\Omega(-1)^{p+1}$ [13] in the context of IBVP (17). Accordingly, the breakdown time is now given by

$$t_\infty\equiv\frac{2}{\sigma}\ln\left[\frac{\Omega(-1)^p}{\Omega(-1)^p+\alpha^*}\right],\tag{19}$$

which we observe is positive *only* if the conditions of Case (V) are satisfied.

4.2. Scheme construction

To simplify the analysis, we let $v=V+v^+$, where in terms of V we now have $[\![V]\!]=0$, $[\![V_x]\!]=[\![v_x]\!]$, $[\![V_t]\!]=[\![v_t]\!]$, and $U=\mathfrak{C}(0,v^+)$, and where

$$\mathfrak{C}(V,v^+)\equiv\mathscr{C}(V+v^+)=\sqrt{1+3\varepsilon^2\beta(V+v^+)^2}.\tag{20}$$

Next, we modify the finite difference scheme used by Jordan and Puri [13], who studied the undamped, i.e., $\sigma\to 0$, case of Eq. (7), to include a centered-difference representation of the damping term. This results in the discretized equation of motion, now expressed in terms of V,

$$\frac{V_m^{k+1}-2V_m^k+V_m^{k-1}}{(\Delta t)^2}+\sigma\left[\frac{V_m^{k+1}-V_m^{k-1}}{2(\Delta t)}\right]-[1+3\varepsilon^2\beta(V_m^k+v^+)^2]\left[\frac{V_{m+1}^k-2V_m^k+V_{m-1}^k}{(\Delta x)^2}\right]$$
$$=3\varepsilon^2\beta(V_m^k+v^+)\left[\frac{(V_{m+1}^k-V_{m-1}^k)^2}{2(\Delta x)^2}\right].\tag{21}$$

Here, $V_m^k\approx V(x_m,t_k)$ and the mesh points (x_m,t_k) are given by $x_m=m(\Delta x)$, for each $m=0,1,2,\ldots,M$, and $t_k=k(\Delta t)$, for each $k=0,1,2,\ldots,K$, where $M\geqslant 2$ and $K\geqslant 2$ are integers, and the (uniform) spatial- and temporal-step sizes are $\Delta x=1/M$ and $\Delta t=1/K$, respectively. On setting $R=(\Delta t)/(\Delta x)$ and solving for V_m^{k+1}, the most forward time-step approximation, we obtain the (explicit) finite

difference scheme

$$V_m^{k+1} = \left\{ \frac{3}{2} R^2 \varepsilon^2 \beta (V_m^k + v^+)(V_{m+1}^k - V_{m-1}^k)^2 + R^2 [1 + 3\varepsilon^2 \beta (V_m^k + v^+)^2](V_{m+1}^k - 2V_m^k + V_{m-1}^k) + (2V_m^k - V_m^{k-1}) + \frac{\sigma}{2}(\Delta t) V_m^{k-1} \right\} \left[1 + \frac{\sigma}{2}(\Delta t) \right]^{-1}, \tag{22}$$

which holds for each $m = 1, 2, 3, \ldots, M-1$ and $k = 1, 2, 3, \ldots, K-1$, and we note that the scheme's overall truncation error is $O[(\Delta x)^2 + (\Delta t)^2]$.

4.3. Linearized problem: approximate solution

To highlight the effects of the nonlinearities, plots of the solution profile corresponding to the linearized version of IBVP (17), where the equation of motion is the simple damped wave equation (see, e.g., Ref. [28] and those therein)

$$v_{tt} + \sigma v_t - v_{xx} = 0, \tag{23}$$

are also presented. While the exact solution of the linearized problem can be readily determined using, e.g., the Laplace transform method, for the purposes of the present study, however, the following simple expression, which very closely approximates the former for $t \in (0, t_r)$, will be more than adequate:

$$V(x,t) = v(x,t) - v^+ \approx (-1)^{p+1} H(t-x) \exp\left(-\frac{1}{2}\sigma x \right) \sin[\Omega(t-x)]. \tag{24}$$

4.4. Numerical simulations

In Figs. 1–3 we have presented velocity profile plots corresponding to Cases (I), (II), and (V), respectively, where the values taken here for Ω, R, and p are the same as those used in Figs. 1(a) and (b) of Ref. [13]. Additionally, the values of β that we employed were selected both because they fell within the range of such values given in Ref. [17, Fig. 12] and they allow us to generate, using physically consistent values of ε, figures that clearly illustrate the above three cases. In particular, in Fig. 3 we chose ε and β so that t_∞ would be less than, but very close to, t_r. Consequently, the (dimensionless) *discontinuity distance*,

$$x_\infty = \mathfrak{C}(0, v^+) t_\infty = \left(\frac{2\sqrt{1 + 3\varepsilon^2 \beta (v^+)^2}}{\sigma} \right) \ln\left[\frac{\Omega(-1)^p}{\Omega(-1)^p + \alpha^*} \right], \tag{25}$$

corresponding to Fig. 3 is less than, but very close to, the right boundary $x = 1$. And we should point out that $\sigma = 1.0$ was used in Figs. 1–3 simply because it allows the effects of attenuation on the solution profiles to be easily observed.

The three time sequences given depict the evolution of the V vs. x solution profile during Σ's initial transit of the interval $(0, 1)$. The boldface curves correspond to the numerical solution of IBVP (17) and were produced from data sets computed by a simple algorithm which implemented the scheme given in Eq. (22) on a PC running MATHEMATICA (Version 5.0). Interpolations between the points were accomplished using the cubic splin routine built-in to this software package. In addition, so as to illustrate the behavior of $[\![V_x]\!] = V_x^-$, we have in each sub-figure plotted straight line segments, whose slopes were computed using Eq. (18), through the point $(x, V) = (\Sigma(t), 0)$. And to allow for comparisons of the nonlinear vs. linear versions of IBVP (17), we have included plots of Eq. (24) as the broken curves.

Fig. 1 is plotted for $v^+ = 0$ and corresponds to Case (I), where the amplitude of Σ experiences exponential decay over time. Here, we see that the propagation speed $U = \mathfrak{C}(0, 0) = 1$ of Σ, as well as its amplitude $[\![V_x]\!]$,

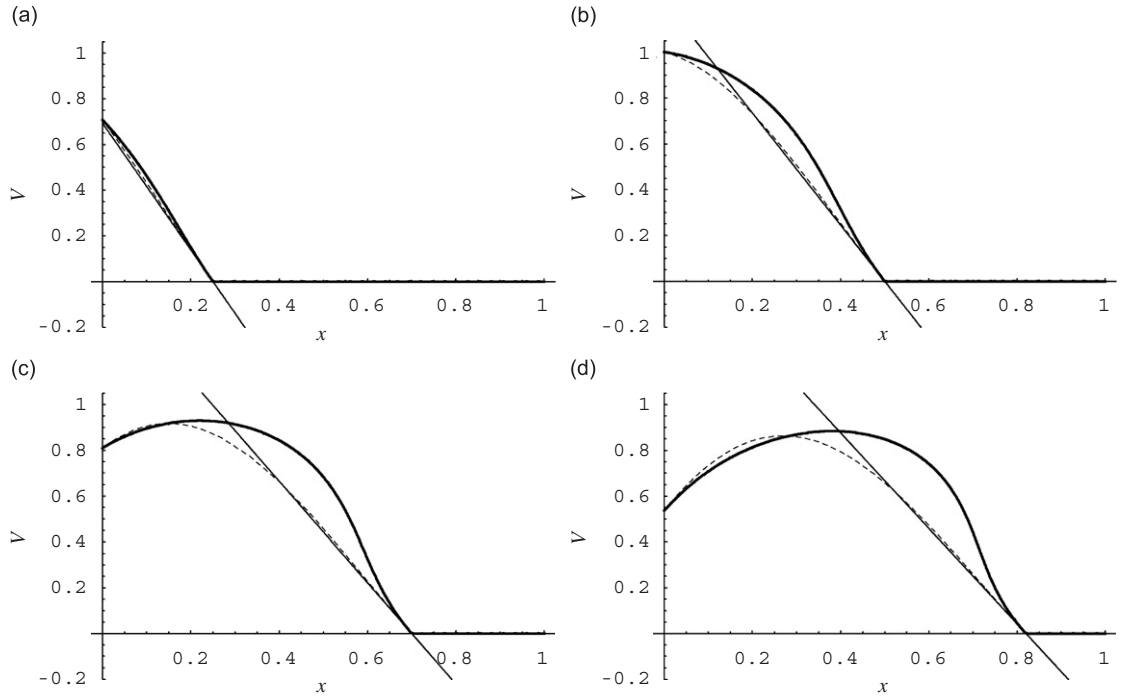

Fig. 1. V vs. x for $p=1$, $v^{+}=0$, $\varepsilon=0.05$, $\beta\approx 140.85$, $\sigma=1.0$, $\Omega=\pi$, $\mathfrak{C}(0,0)=1.0$, $\Delta x=1/2000$, $\Delta t=1/4000$, and $R=1/2$. (a): $t=0.25$, (b): $t=0.50$, (c): $t=0.70$, and (d): $t=0.82$. Bold: numerical solution of IBVP (17). Broken: Eq. (24). Thin-solid: tangent line at $x=\Sigma(t)$ with slope given by Eq. (18).

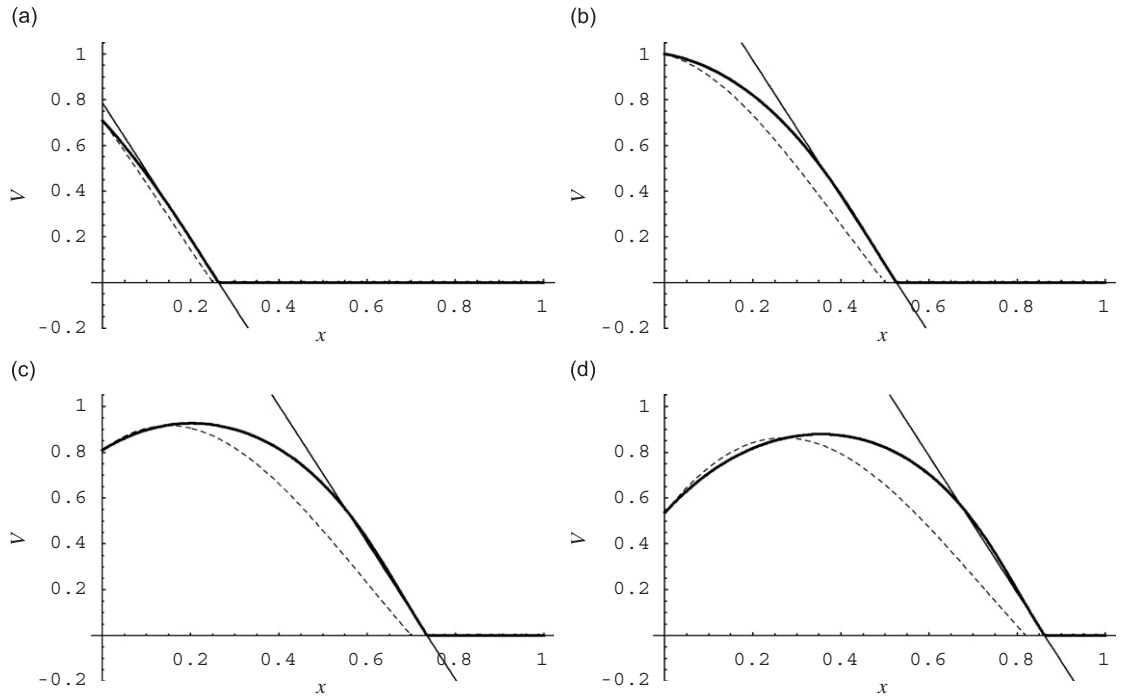

Fig. 2. V vs. x for $p=1$, $v^{+}=0.6$, $\varepsilon=0.03$, $\beta\approx 108.62$, $\sigma=1.0$, $\Omega=\alpha^{*}=\pi$, $\mathfrak{C}(0,0.6)\approx 1.0515$, $\Delta x=1/2000$, $\Delta t=1/4000$, and $R=1/2$. (a): $t=0.25$, (b): $t=0.50$, (c): $t=0.70$, and (d): $t=0.82$. Bold: numerical solution of IBVP (17). Broken: Eq. (24). Thin-solid: tangent line at $x=\Sigma(t)$ with slope given by Eq. (18).

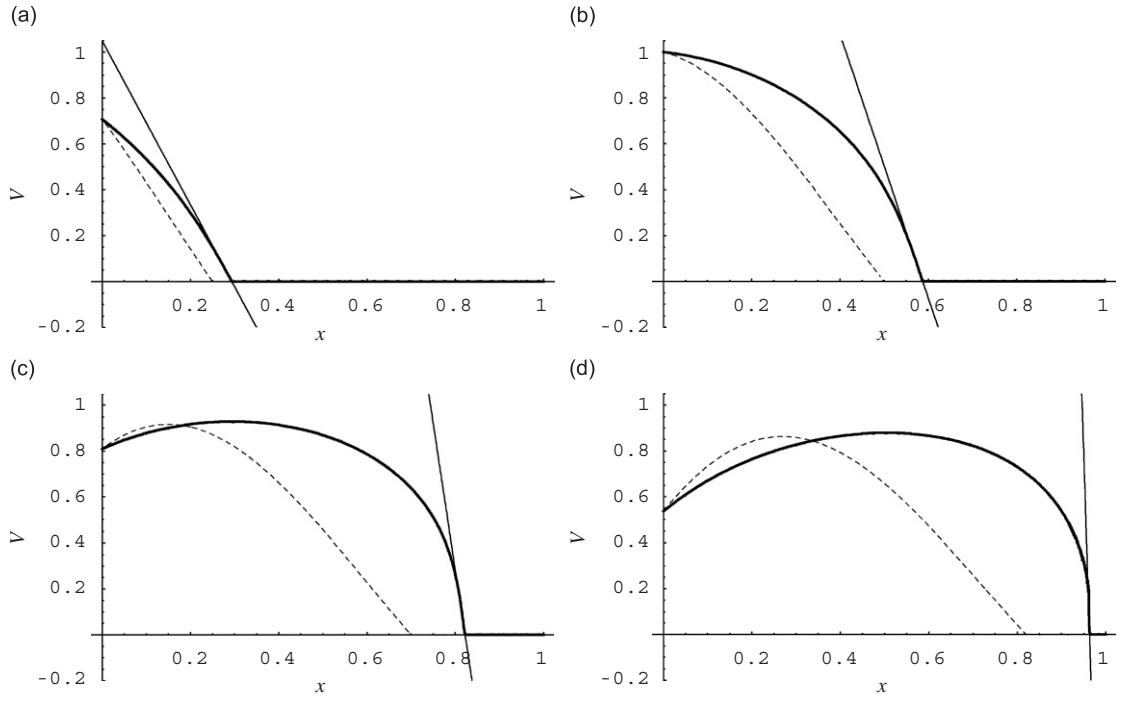

Fig. 3. V vs. x for $p=1$, $v^+=0.6$, $\varepsilon=0.05$, $\beta\approx 140.85$, $\sigma=1.0$, $\Omega=\pi$, $\mathfrak{C}(0,0.6)\approx 1.1749$, $\alpha^*\approx 1.0889$, $t_\infty\approx 0.8511$, $x_\infty\approx 0.9999$, $\Delta x=1/2000$, $\Delta t=1/4000$, and $R=1/2$. (a): $t=0.25$, (b): $t=0.50$, (c): $t=0.70$, and (d): $t=0.82$. Bold: numerical solution of IBVP (17). Broken: Eq. (24). Thin-solid: tangent line at $x=\Sigma(t)$ with slope given by Eq. (18).

are equal in the nonlinear and linear solution curves, as they should be for $v^+=0$. We also see that both solution curves are, as expected, attenuated.

From Fig. 2 we observe, as predicted in Case (II), that the slope of the profile at the wavefront is constant, specifically, $[\![V_x]\!]=V_x^-=-\pi$. Note also that while the propagation speed of Σ corresponding to the nonlinear solution is greater than that of the linear solution, i.e., greater than unity, the former profile does not appear to undergo distortion, but like its linear counterpart it clearly suffers attenuation.

In contrast, Fig. 3, which captures ~95% of the amplitude blow-up predicted in Case (V), clearly shows that there is a rapid increase in $|[\![V_x]\!]|$ as $t\to t_\infty$, along with attenuation of the solution curve. The former is, of course, due to the amplitude-dependence of the wave speed (see Eq. (20), where $\mathfrak{C}(0,0.6)>1$ is evident from a comparison of the nonlinear and linear profiles, while the latter results from the (damping) term v_t. What is most interesting, however, can be seen in the last frame of Fig. 3. There, the profile appears to be preparing to "break," in much the same way as in the corresponding undamped case (see Ref. [13, Fig. 1(b)]). Such behavior, which is only possible when $v^+\neq 0$, strongly suggests that a vortex sheet is forming.

Finally, because of the relatively slow decay involved, whereby significant variations in the waveform do not occur over the course of Σ's initial transit, sequences for Cases (III) and (IV) have been omitted.

5. Summary and discussion

We have examined the evolution of transverse acceleration waves on a nonlinear string whose motion takes place in a resisting medium. It was shown that the primary effect of external damping is to increase, with respect to the undamped case, the rate at which growth and/or decay of the wave's amplitude takes place. Specifically, with no damping the rate is algebraic [13]; but when external damping is included the rate becomes exponential. In addition, we found that v^+ must be nonzero if finite-time blow-up is to be possible, a situation which also arises in shear flows of certain nonlinear viscoelastic fluids [6]. In contrast, taking $v^+=0$ yields a jump amplitude identical to that of Eq. (23), the linearized equation of motion (see Eq. (14) and Case (I)). What's more, we showed that with external damping included, the constant amplitude solution

$a(t) = \alpha^*$ (see Case (II)) requires $v^+ \neq 0$ *and* $a(0) = \alpha^*$, which is unlike the undamped case where such a solution is obtained by taking $v^+ = 0$ [13]. However, we also showed that $a(t) = \alpha^*$ is an unstable equilibrium solution of Eq. (13); see the Appendix.

Lastly, a series of numerical simulations of acceleration waves on a finite string was used to graphically illustrate Cases (I), (II), and (V). It was shown that, with regard to the V vs. x solution profiles, the main effect of external damping here was the introduction of attenuation.

Acknowledgments

The author would like to thank the three anonymous referees for their extremely helpful comments and suggestions. P.M. Jordan was supported by ONR/NRL funding (PE 061153N).

Appendix A. Qualitative analysis of jump amplitude equation

Although we have obtained the exact solution of Eq. (13), it is nevertheless instructive to investigate the steady-state behavior of the acceleration wave amplitude using qualitative methods. To this end, let us (briefly) re-examine the stability characteristics of the equilibrium solutions $\bar{a} = \{0, \alpha^*\}$, which correspond to the roots of the quadratic equation

$$\bar{a}\left(1 - \frac{\bar{a}}{\alpha^*}\right) = 0, \tag{A.1}$$

where we now regarded α^* as a function of v^+ (see Eq. (15)).

Referring the reader to the excellent books by Hale and Koçak [29] and Strogatz [30] for the details, it can be readily established that

$$\bar{a} = \begin{cases} 0 & \begin{cases} \text{Stable}: & v^+ \neq 0, \\ \text{Unstable}: & \emptyset, \end{cases} \\ \alpha^* & \begin{cases} \text{Stable}: & \emptyset, \\ \text{Unstable}: & v^+ \neq 0, \end{cases} \end{cases} \tag{A.2}$$

where we note that $v^+ = 0$ has been excluded.

The stability diagram presented in Fig. A1, which was generated by plotting α^* vs. v^+ (bold-broken curves) along with the zero solution (solid bold lines), clearly illustrates the situation described by Eq. (A.2). In particular, we see that $\bar{a} = \alpha^*$ is always unstable while $\bar{a} = 0$ is always stable.[2] Additionally, we observe that a bifurcation does *not* occur; i.e., there is no "swapping" of stability between the two equilibria. Note also the Roman numerals appearing in Fig. A1; they are used to denote the regions/curves corresponding to Cases (II)–(V).

And for completeness, we observe that the (bold-broken) curves that appear in the 3rd and 1st Quadrants of Fig. A1 have as their stationary points

$$v^+_{1,2} = \frac{\mp 1}{\varepsilon\sqrt{3\beta}}, \tag{A.3}$$

respectively. Consequently, it can be shown that

$$\max_{v^+ < 0}(\alpha^*) = \alpha^*\Big|_{v^+ = v^+_1} = \frac{-\sigma}{\varepsilon\sqrt{3\beta}} < 0, \tag{A.4}$$

which corresponds to the curve in the 3rd Quadrant, and

$$\min_{v^+ > 0}(\alpha^*) = \alpha^*\Big|_{v^+ = v^+_2} = \frac{\sigma}{\varepsilon\sqrt{3\beta}} > 0, \tag{A.5}$$

[2] More precisely, an asymptotically stable, hyperbolic equilibrium point for all $v^+ \neq 0$; see Ref. [29].

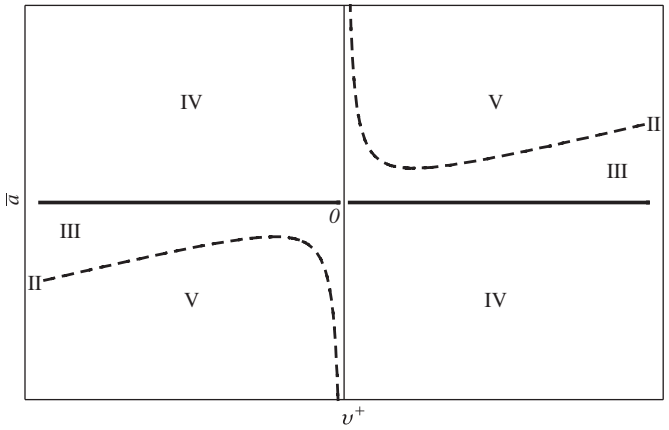

Fig. A1. Stability diagram for the acceleration wave amplitude, where $v^+ \neq 0$ is assumed. Here, the two bold-broken curves correspond to Case (II); the regions in the 1st and 3rd Quadrants that are bounded by these curves and the coordinate axes correspond to Case (III), with the remaining regions of these two quadrants corresponding to Case (V); and the entire 2nd and 4th Quadrants correspond to Case (IV). Bold-solid: stable equilibria. Bold-broken: unstable equilibria.

which corresponds to the curve in the 1st Quadrant. Thus, we see that the critical amplitude, which is never zero, is restricted to one of two semi-infinite intervals, namely,

$$\alpha^* \in \begin{cases} \left[\dfrac{\sigma}{\varepsilon\sqrt{3\beta}}, +\infty\right), & v^+ > 0, \\ \left(-\infty, \dfrac{-\sigma}{\varepsilon\sqrt{3\beta}}\right], & v^+ < 0. \end{cases} \tag{A.6}$$

References

[1] C. Truesdell, R.A. Toupin, The classical field theories, in: S. Flügge (Ed.), *Handbuch der Physik*, Vol. III/1, Springer, Berlin, 1960, pp. 491–529.
[2] M.F. McCarthy, Singular surfaces and waves, in: A.C. Eringen (Ed.), *Continuum Physics*, Vol. II, Academic Press, London, 1975, pp. 449–521.
[3] J.N. Johnson, R. Cheret, *Classic Papers in Shock and Compression Science*, Springer, New York, 1998.
[4] P.J. Chen, Growth and decay of waves in solids, in: S. Flügge, C. Truesdell (Eds.), *Handbuch der Physik*, Vol. VIa/3, Springer, Berlin, 1973, pp. 303–402.
[5] J.D. Logan, *An Introduction to Nonlinear Partial Differential Equations*, Wiley, New York, 1994 (Chapter 5).
[6] B.D. Coleman, M.E. Gurtin, On the stability against shear waves of steady flows of non-linear viscoelastic fluids, *Journal of Fluid Mechanics* 33 (1968) 165–181.
[7] B.D. Coleman, M.E. Gurtin, Growth and decay of discontinuities in fluids with internal state variables, *Physics of Fluids* 10 (1967) 1454–1458.
[8] Y.B. Fu, N.H. Scott, The transition from acceleration wave to shock wave, *International Journal of Engineering Science* 29 (1991) 617–624.
[9] I. Müller, T. Ruggeri, Extended thermodynamics, in: C. Truesdell (Ed.), *Springer Tracts in Natural Philosophy*, Vol. 37, Springer, New York, 1993, pp. 148–152.
[10] G. Saccomandi, Acceleration waves in a thermo-microstretch fluid, *International Journal of Non-Linear Mechanics* 29 (1994) 809–817.
[11] R. Quintanilla, B. Straughan, A note on discontinuity waves in type III thermoelasticity, *Proceedings of the Royal Society A* 460 (2004) 1169–1175.
[12] P.M. Jordan, C.I. Christov, A simple finite difference scheme for modeling the finite-time blow-up of acoustic acceleration waves, *Journal of Sound and Vibration* 281 (2005) 1207–1216.
[13] P.M. Jordan, A. Puri, Growth/decay of transverse acceleration waves in nonlinear elastic media, *Physics Letters A* 341 (2005) 427–434.
[14] I. Christov, P.M. Jordan, C.I. Christov, Nonlinear acoustic propagation in homentropic perfect gases: a numerical study, *Physics Letters A* 353 (2006) 273–280.

[15] M. Ciarletta, B. Straughan, Poroacoustic acceleration waves, *Proceedings of the Royal Society A* 462 (2006) 3493–3499.
[16] J. Jaisaardsuetrong, B. Straughan, Thermal waves in a rigid heat conductor, *Physics Letters A* 366 (2007) 433–436.
[17] D.W. Oplinger, Frequency response of a nonlinear stretched string, *The Journal of the Acoustical Society of America* 32 (1960) 1529–1538.
[18] G.F. Carrier, On the non-linear vibration problem of the elastic string, *Quarterly of Applied Mathematics* 3 (1945) 157–165.
[19] J.D. Cole, C.B. Doughererty, J.H. Huth, Constant-strain waves in strings, *Journal of Applied Mechanics (Transactions of the ASME)* (1953) 519–522.
[20] E.W. Lee, Non-linear forced vibrations of a stretched string, *British Journal of Applied Physics* 8 (1957) 411–413.
[21] I.-S. Liu, M.A. Rincon, Effects of moving boundaries on the vibrating elastic string, *Applied Numerical Mathematics* 47 (2003) 159–172.
[22] J.M. Greenberg, R.C. MacCamy, V.J. Mizel, On the existence, uniqueness, and stability of solutions of the equation $\sigma'(u_x)u_{xx} + \lambda u_{xtx} = \rho_0 u_{tt}$, *Journal of Mathematics and Mechanics* 17 (1968) 707–728.
[23] G.E. Mase, *Continuum Mechanics*, McGraw-Hill, New York, 1970 (Chapter 9).
[24] R.B. Guenther, J.W. Lee, Partial Differential Equations of Mathematical Physics and Integral Equations, Dover, Mineola, NY, 1996, pp. 206–208.
[25] G.B. Whitham, Linear and Nonlinear Waves, Wiley, New York, 1974, pp. 26–30.
[26] D.R. Bland, *Wave Theory and Applications*, Oxford University Press, Oxford, 1988.
[27] B.D. Coleman, J.M. Greenberg, M.E. Gurtin, Waves in materials with memory V. On the amplitude of acceleration waves and mild discontinuities, *Archive for Rational Mechanics and Analysis* 22 (1966) 333–354.
[28] R.E. Mickens, P.M. Jordan, A positivity-preserving nonstandard finite difference scheme for the damped wave equation, *Numerical Methods for Partial Differential Equations* 20 (2004) 639–649.
[29] J. Hale, H. Koçak, *Dynamics and Bifurcations*, Springer, New York, 1991 (Chapters 1–2).
[30] S.H. Strogatz, *Nonlinear Dynamics and Chaos*, Addison–Wesley, Reading, MA, 1994 (Chapters 2–3).